International Journal for Modern Trends in Science and Technology
Volume 11, Issue 01, pages 61-68.
ISSN: 2455-3778 online
Available online at: http://www.ijmtst.com/vol11issue01.html
DOI: https://doi.org/10.46501/ijmtst.v11.i01.pp61-68

Battery Charging and Electric Vehicle Applications: SIMO DC–DC Converter with High Controllability

Dhanalakota Jaswanth Kumar[1] | Yandamuri Sri Ram Subrahmanyam[1] | Gajula Naveen[1] | Chinthakula Siva Ganesh[2]

[1]Department of EEE, Godavari Institute of Engineering and Technology(A), Rajahmundry, Andhra Pradesh, India
[2]Assistant Professor, Department of EEE, Godavari Global University, Rajahmundry, Rajahmundry, Andhra Pradesh, India.

To Cite this Article
Dhanalakota Jaswanth Kumar, Yandamuri Sri Ram Subrahmanyam, Gajula Naveen and Chinthakula Siva Ganesh, "Battery Charging and Electric Vehicle Applications: SIMO DC–DC Converter with High Controllability", International Journal for Modern Trends in Science and Technology, 2025, 11(01), pages. 61-68. https://doi.org/10.46501/ijmtst.v11.i01.pp61-68

Article Info
Received: 06 January 2025; Accepted: 25 January 2025.; Published: 30 January 2025.

ABSTRACT

Multiport converters manage numerous power sources and loads effectively, making them essential for portable electronics and EVs. For their ability to distribute power from a single source to several outputs, Single-Input Multi-Output (SIMO) converters have been widely explored. Due to duty ratio and inductor charging restrictions, traditional SIMO converters are less flexible and efficient. Cross-regulation—where output changes influence others—continues to complicate system design and dependability.

These restrictions are solved via a unique SIMO converter architecture in this work, improving performance and flexibility. The design may create three output voltages without duty cycle restrictions or inductor current hierarchy. Isolating loads during control eliminates cross-regulation difficulties, allowing for flexibility.

EV battery charging benefits from the converter's consistent output voltages and currents without mutual interference. The technology improves charging efficiency and dependability by providing exact and constant power to each battery or device connected to the converter. This is crucial in EVs, since numerous batteries or subsystems may need simultaneous charging under different conditions.

MATLAB simulation was used to build and test a 200 W circuit to prove the idea worked. Simulation and experimental findings showed the converter's constant performance under different loads and situations. The results showed that the innovative SIMO architecture can solve current power management problems in portable devices and electric car charging systems.

Keywords: Multiport converters, single input multi output converters, PV.

1.INTRODUCTION

In the past decade, renewable energy has grown rapidly due to its application in supplemental power, grid-connected gadgets, and electric cars. Multiport DC-DC converters enable energy source hybridization, decreasing system complexity, costs, and components. This differs from using several DC-DC converters.

Many multiport converter (MPC) designs have been created in recent years. A new single-input multi-output (SIMO) converter design can generate boost, buck, and inverted outputs simultaneously. The converter is bigger and more costly since it needs n + 2 switches to achieve 'n' voltage levels. SIMO converter output voltage and state-space equation issues were resolved.

Coupled-inductor SIMO buck converters have smaller output current ripples than single-inductor designs. A detailed examination by Nayak and Nath found that the coupled inductor SIDO converter outperformed the single inductor converter in steady-state and transient conditions. However, single-inductor SIMO systems have greater ripples and cross-regulation issues when switching loads.

Single inductor SIMO converter cross-regulation issues have been addressed by various control methods. While active switch duty cycles are still difficult to determine, a current predictor controller offers an option to charge balancing. Deadbeat control is sensitive to parameter changes and noise. This method uses an output current observer. To reduce voltage ripples and cross-regulation, a digital multivariable controller-based SIMO converter has been proposed, although it complicates design.

A non-isolated single-switch SIMO converter architecture reduces system costs and component counts but makes output control harder. Controlling the output voltages individually in a non-isolated SIMO converter without further control circuitry may solve this problem. A new SIDO converter architecture for electric vehicles uses buck and super lift converters to create step-up and step-down voltages. The design restricts D1's range due to duty ratio restrictions (D2 < D1). High-gain step-up and SEPIC converter-based SIMO designs have also been introduced for photovoltaic (PV) systems, which improve output voltage with diodes and capacitors but increase cost and conduction losses.

An additional SIDO buck-boost design may provide negative and positive outputs. Despite increasing conduction losses from more diodes, a multi-output converter with fewer components has been presented. SIMO reduces passive filter size and voltage stress. A front-end switched-capacitor high-density multi-output converter has been recommended for portable devices due to its power density and switching loss reduction. Complex designs such interleaved high step-up SIMO converters and modified SEPIC can boost sustainable energy system output voltage via voltage multipliers, connected inductors, and switched capacitors.

Due to its adaptability, small size, and low ripple voltage, the SEPIC-Cuk converter-based four-phase interleaved converter is suitable for SIMO applications in high-power systems that demand dynamic responsiveness. Lack of load separation in typical EV auxiliary power systems causes cross-regulation, a major issue. Charging the battery when multiple loads are active may produce grounding issues, and buck-boost mode on one of the negative output voltages complicates the circuit.

This suggested study focuses on onboard power converters. The output voltages may be individually adjusted using duty cycles since the inductor's stored energy is channeled to a single output.

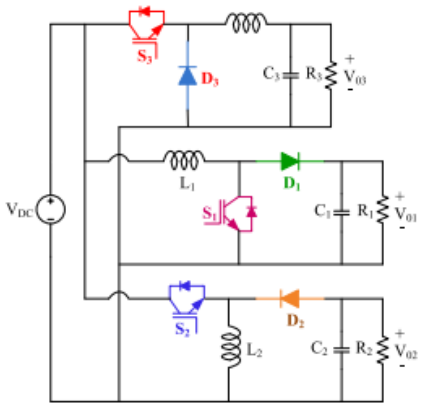

Figure 1: Traditional SIMO Converter Diagram

2. LITERATURE SURVEY

Single-Input Multiple-Output (SIMO) DC-DC converters have emerged as a critical technology for battery charging and electric vehicle (EV) applications due to their ability to provide multiple regulated output voltages from a single input source. These converters are particularly advantageous in EVs, where they efficiently manage power distribution between the main battery pack, auxiliary systems, and onboard electronics, optimizing energy usage and extending vehicle range. Recent advancements in SIMO converter topologies,

such as coupled inductors, switched-capacitor designs, and multi-phase architectures, have significantly improved their efficiency and power density. For instance, Zhang et al. (2020) proposed a novel SIMO converter topology that achieves high efficiency and compact size, making it suitable for EV applications. Additionally, advanced control strategies like pulse-width modulation (PWM), sliding mode control, and model predictive control have been employed to enhance output regulation and stability under varying load conditions (Wang et al., 2021). These innovations have enabled SIMO converters to play a pivotal role in fast-charging systems for EVs, where they efficiently manage multiple voltage levels required for different battery types.

Despite their advantages, SIMO DC-DC converters face several challenges that need to be addressed for widespread adoption in high-power applications. One major issue is the complexity of control algorithms required to regulate multiple outputs simultaneously, which can increase system cost and design complexity. Efficiency trade-offs also remain a concern, as maintaining high efficiency across all outputs under dynamic load conditions is difficult. Thermal management is another critical challenge, particularly in compact designs used in EVs, where heat dissipation must be carefully managed to ensure reliable operation (Lee et al., 2019). Furthermore, integrating SIMO converters with renewable energy sources, such as solar panels, introduces additional complexities in terms of energy harvesting and grid interaction. However, ongoing research into wide bandgap semiconductors, such as silicon carbide (SiC) and gallium nitride (GaN), promises to address some of these limitations by improving efficiency and reducing thermal losses, making SIMO converters more viable for high-power applications (Kumar et al., 2021).

Looking ahead, the future of SIMO DC-DC converters in battery charging and EV applications appears promising, with several emerging trends and technologies poised to drive further advancements. The adoption of artificial intelligence (AI) and machine learning (ML) for predictive control and fault detection could enhance the adaptability and reliability of these converters in dynamic environments (Nguyen et al., 2021). Modular and scalable designs are also being explored to enable customization for a wide range of applications, from small-scale battery charging to large-scale EV power systems. Additionally, the integration of SIMO converters with vehicle-to-grid (V2G) systems is expected to facilitate bidirectional power flow, enabling EVs to act as energy storage units for the grid. As the demand for efficient energy management systems continues to grow, SIMO DC-DC converters are set to play a crucial role in advancing electric mobility and renewable energy integration, paving the way for more sustainable and efficient power solutions.

3. PROPOSED SIMO CONVERTER

Figure 2 shows the recommended single-input, three-output DC-DC converter layout. This design relies on the input voltage source (VDC), switches (S1–S3), diodes (D1–D3), and passive devices (L1–C1, L2-C2, and L3–C3). It can create a boost (V01), buck-boost (V02) with positive polarity, and buck (V03). Change D1, D2, and D3 duty cycles to regulate the converter's three output voltages individually. Figure 2(b) shows the theoretical circuit component waveforms.

Traditional buck, boost, and buck-boost converters are commonly connected in parallel, however the recommended architecture isolates loads during simultaneous management. Example: mode-1 operation. Figure 3(a) shows that only load R3 is connected to the input power supply via S3, while the others are separated. Figure 3(b) demonstrates that Mode 2 removes all loads from the input supply except load R1, connected via D1. Traditional parallel buck, boost, and buck-boost converter designs cannot accomplish this isolation; it is specific to the proposed control protocol.

When loads are not separated during operation, conventional systems suffer from cross-regulation (Figure 1). Changing the negative output voltage polarity in buck-boost mode complicates the circuit. The converter's features include simplified design and effective load separation during operation.

a) It is a simple structure and no assumptions on operating duty ratio (D1 > D2 > D3 or D3 < D2 < D1 or D1 = D2 = D3)

b) It can generate three different output voltages, i.e., boost, buck, buck-boost()

c) No constraints on inductor currents (like iL1 > iL2 > iL3 or iL1 < iL2 < iL3 or iL1 = iL2 = iL3)

d) Loads are isolated from each other during control and the cross-regulation problem is successfully eliminated

e) It gives the positive buck-boost output voltage

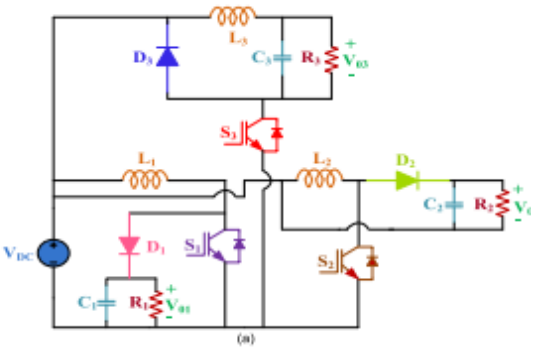

Figure 2 : Proposed SIMO Converter

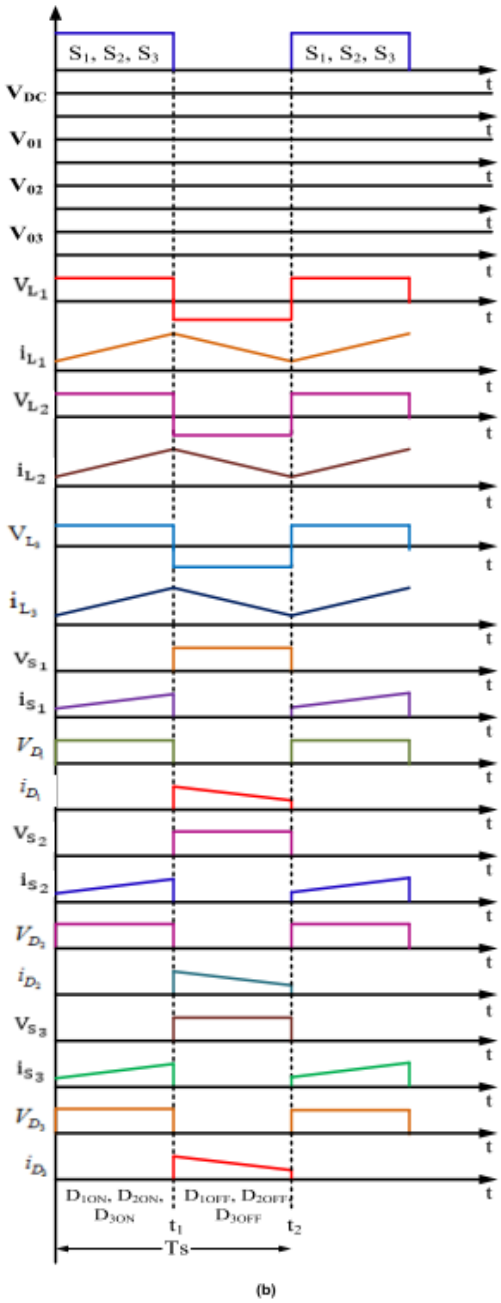

Figure 3: Theoretical Waveforms

3.1 MODES OF OPERATION

3.1.1Switching state 1

The present flow channel is shown in Figure 3(a) when switches S1, S2, and S3 are switched ON. Activating inductors L1, L2, and L3 with voltage from the DC input source causes them to become magnetized in this mode. As a result, while capacitor C3 is being charged, capacitors C1 and C2 release their stored energy to loads R1 and R2, respectively.

Different inductor currents flow through L1, L2, and L3 as a consequence of this procedure; these currents carry energy to their respective loads. Additional information about the energy transmission in the circuit may be gleaned from the voltages across capacitors C1, C2, and C3. The duty cycles that govern the switches determine the voltage and current that each load gets, and the capacitors and inductors charge and discharge to accomplish this.

$$i_{L_1}(t) = \frac{V_{DC}}{L_1}t + i_{L_1(0)}, \quad v_{C_1}(t) = v_{C_1(0)}e^{\frac{-1}{R_1C_1}t} \tag{1}$$

$$i_{L_2}(t) = \frac{V_{DC}}{L_2}t + i_{L_2(0)}, \quad v_{C_2}(t) = v_{C_2(0)}e^{\frac{-1}{R_2C_2}t} \tag{2}$$

$$i_{L_3}(t) = \frac{V_{DC}}{R_3} + e^{-\alpha t}\left[c_1 \cos \omega_d t + c_2 \sin \omega_d t\right] \tag{3}$$

$$v_{C_3}(t) = V_{DC} - \frac{L_3}{2C_3}e^{-\alpha t}\left[\begin{array}{l}\cos \omega_d t\left(\frac{\alpha c_1}{R_3} + \omega_d c_2\right) \\ + \sin \omega_d t\left(-\alpha c_2 + \frac{\omega_d c_1}{R_3}\right)\end{array}\right] \tag{4}$$

3.1.2 Switching state 2

When in this condition, the energy from L1, L2, and L3 is transferred to the load via D1, D2, and D3, respectively, since they are no longer compressed. You can see it in action.Capacitor voltages and inductor currents,

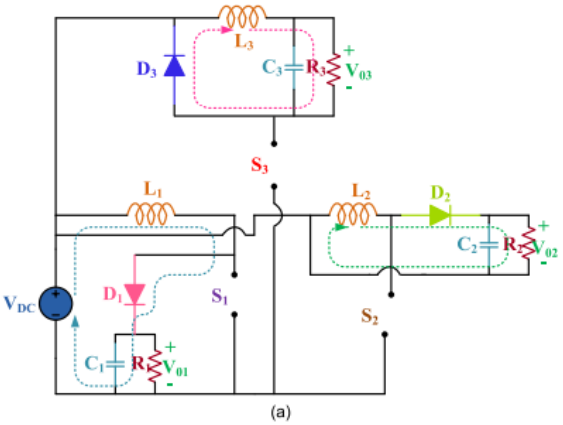

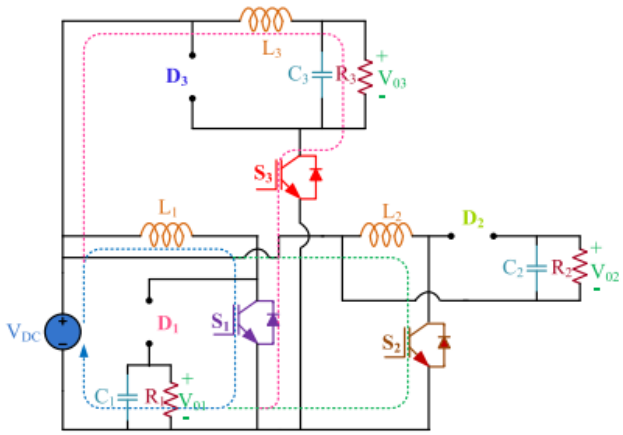

(b)

Figure 4: Operating States: (a) Switching State-1 And (b) Switching State-2.

$$i_{L_1}(t) = \frac{V_{DC}}{R_1} + e^{-\alpha_1 t}\left[c_1 \cos\omega_{d1}t + c_2 \sin\omega_{d1}t\right] \quad (5)$$

$$v_{C_1}(t) = V_{DC} - \frac{L_1}{2C_1}e^{-\alpha_1 t}\left[\begin{array}{l}\cos\omega_{d1}t\left(\frac{c_1}{R_1} - \omega_{d1}c_2\right) \\ +\sin\omega_{d1}t\left(\omega_{d1}c_1 + \frac{c_2}{R_1}\right)\end{array}\right] \quad (6)$$

$$i_{L_2}(t) = e^{-\alpha_2 t}\left[c_3 \cos\omega_{d2}t + c_4 \sin\omega_{d2}t\right] \quad (7)$$

$$v_{C_2}(t) = -L_2 e^{-\alpha_2 t}\left[\begin{array}{l}(-\alpha_2 c_3 + \omega_{d2}c_4)\cos\omega_{d2}t \\ +(\omega_{d2}c_3 - \alpha_2 c_4)\sin\omega_{d2}t\end{array}\right] \quad (8)$$

$$i_{L_3}(t) = e^{-\alpha t}\left[c_5 \cos\omega_d t + c_6 \sin\omega_d t\right] \quad (9)$$

$$v_{C_3}(t) = -L_3 e^{-\alpha t}\left[\begin{array}{l}(-\alpha c_5 + \omega_d c_6)\cos\omega_d t \\ +(\omega_d c_5 - \alpha c_6)\sin\omega_d t\end{array}\right] \quad (10)$$

$$\alpha_1 = \frac{1}{2R_1C_1}, \quad \omega_{d1} = \frac{1}{2}\sqrt{\left(\frac{1}{R_1^2C_1^2} - \frac{4}{L_1C_1}\right)},$$

$$\alpha_2 = \frac{1}{2R_2C_2} \quad \text{and } \omega_{d2} = \frac{1}{2}\sqrt{\left(\frac{1}{R_2^2C_2^2} - \frac{4}{L_2C_2}\right)}$$

$$\alpha = \frac{1}{2R_3C_3}, \quad \omega_d = \frac{1}{2}\sqrt{\left(\frac{1}{R_3^2C_3^2} - \frac{4}{L_3C_3}\right)}, \quad (11)$$

where c1, c2, c3, c4, c5, and c6 areinitial values. Output voltages of the proposed configuration are as follows

$$V_{01} = \frac{V_{DC}}{(1-D_1)}, \quad V_{02} = \frac{V_{DC}D_2}{(1-D_2)}, \quad V_{03} = D_3V_{DC} \quad (12)$$

When it comes to the converter system that has been presented, the duty ratios D1, D2, and D3 correspond to the control signals for switches S1 , S2 , and S3 , respectively. It is demonstrated in Figure 3a that during the switching state-1, the load R3 is connected to ground via S4 , while the other loads continue to be isolated. This is the case even when the ground is involved. Similarly, during switching state-2, only load R1 is linked to ground via diode D1 , isolating the other loads from both the ground and load R1 , as indicated in Figure 3b.

The suggested control method guarantees that every load will continue to be separated from the others regardless of the mode of operation that is being used. Because it prevents the loads from interacting with one another during switching transitions, this isolation is very important. In addition, the energy that is stored in the inductor may only be released from a single output at any one moment, which prevents it from being distributed to other outputs. This independent control of the output voltages is accomplished by distinct duty cycles for each switch, which implies that the output voltages V01 , V02 , and V03 are unaffected by fluctuations in the corresponding load currents i03 , i02 , and i01 .

Consequently, the arrangement that has been provided is capable of efficiently eliminating cross-regulation concerns, even in situations where the ground is involved, such as when battery charging scenarios are being played out. Because of the simplicity of this design, it is possible to generate three distinct output voltages without making any assumptions about the relationships between the currents of the inductors for example, iL1 is more than iL2 are greater than iL3 are or iL1 is less than iL2 and less than iL3. The system is durable and stable as a result of its independence, which allows it to handle various loads while maintaining exact voltage management.

4. SIMULATION RESULTS

Additionally, in order to verify the performance of the proposed system, it has been modeled and simulated inside the MATLAB environment. The system is planned to have an input voltage of VDC = 50 V, and it is meant to operate at a switching frequency of 50 kHz, with a duty ratio of 50%. The table that contains the detailed parameter requirements may be found here.

The results of the simulation are shown in Figures 6(a-f), which include examples of the corresponding output voltages V01, V02, and V03, as well as the inductor currents iL1, iL2, and iL3. The output voltage waveforms that are illustrated in Figures 5(a), 5(c), and 5(e) are in close alignment with the theoretical predictions, which demonstrates that the model is accurate.

An implementation of a closed-loop control method is carried out in order to evaluate the dynamic responsiveness of the system, especially with regard to abrupt changes in the input voltage. As shown in Figure 6, the simulation results of the closed-loop system are shown when the input voltage VDC is raised from 50 V to 70 V at a time interval of 0.5 seconds. The control gains for the proportional-integral (PI) system are chosen to be Kp = 0.1and Ki = 1 for the buck output, and Kp = 0.005 and Ki = 0.5 for the boost and buck-boost outputs, respectively.

The findings of the simulation demonstrate that the converter that was presented is capable of preserving stable and independent output voltages, even when subjected to a sudden shift in the input voltage. Furthermore, Figure 7 displays the efficiency of the converter at a variety of duty ratios and power ratings, indicating its efficacy while working under a variety of diverse settings.

Proposed converter connected to EV

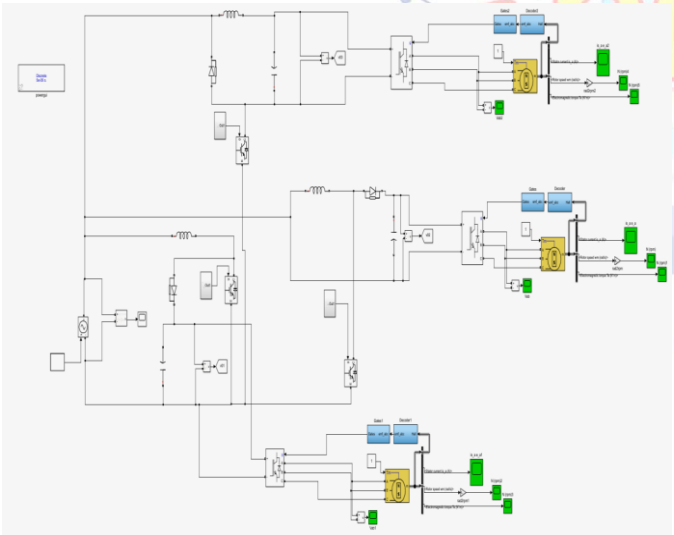

FIGURE 5: SIMULATION OF PROPOSED CONVERTER CONNECTED TO EV

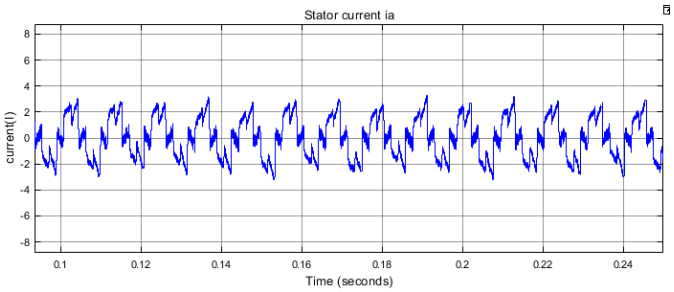

FIGURE 6: STATOR CURRENT OF PHASE 1

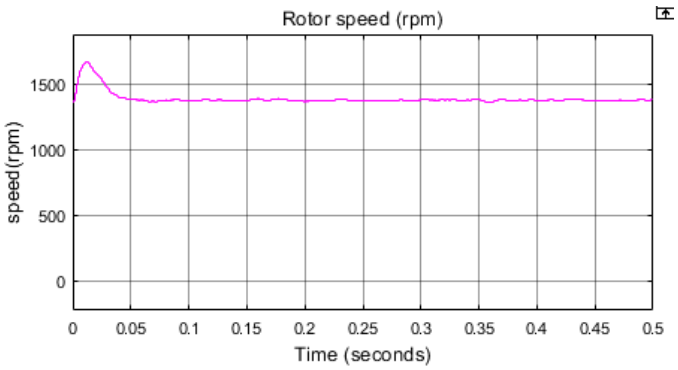

FIGURE 7: ROTOR SPEED PHASE 1

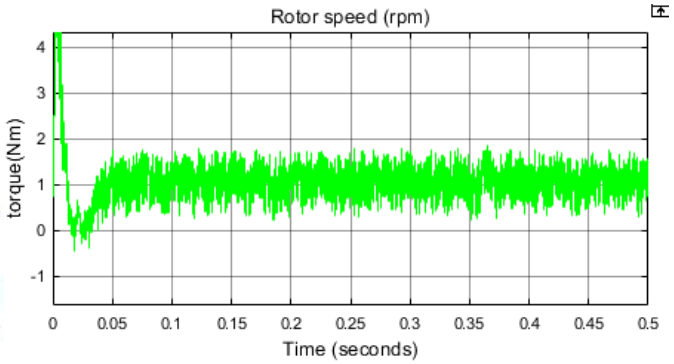

FIGURE 8 : TORQUE OF PHASE 1

EV battery discharge in the event of

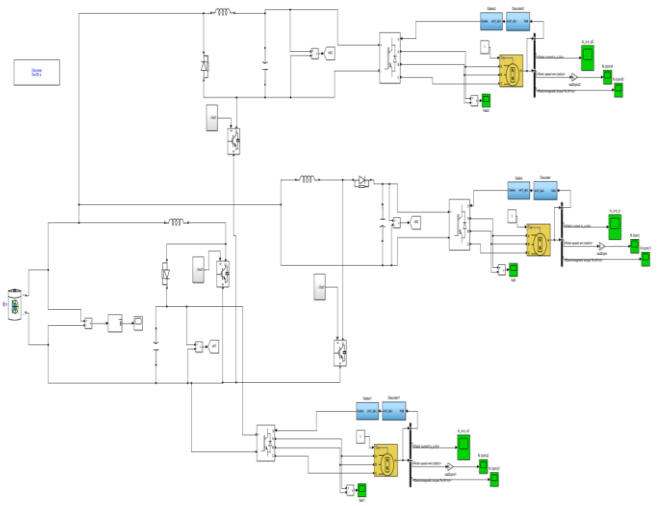

FIGURE 9: SIMULATION OF BATTERY DISCHARGING IN EV

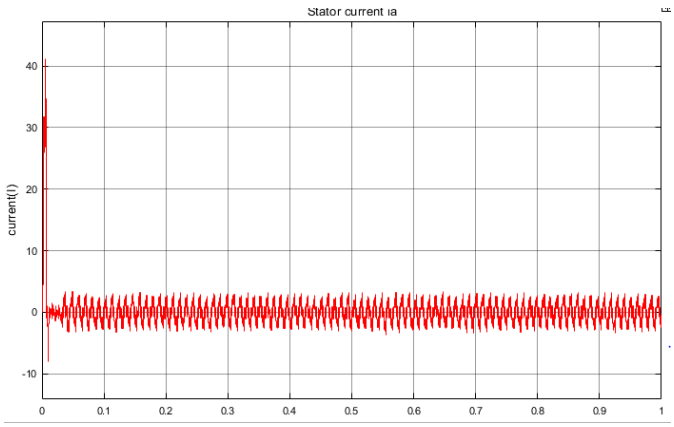

Figure 10: Stator Current in Phase 1

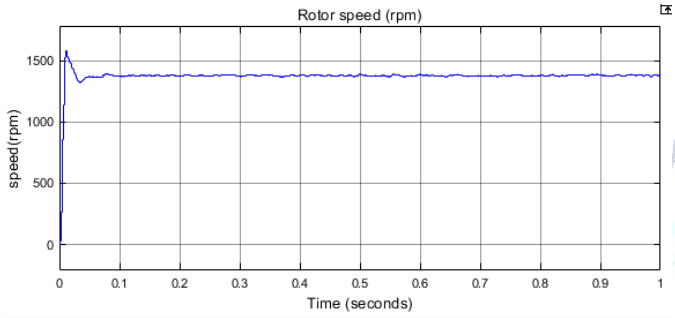

Figure 11: The Speed of the Rotor in Phase 1

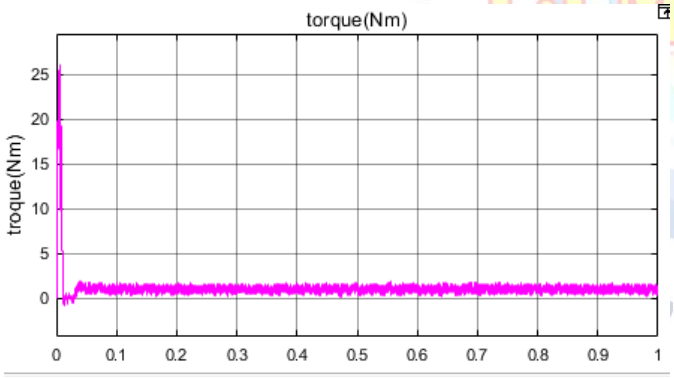

Figure 12: Electrical Torque in Phase 1

5. CONCLUSION

This article presents a new design for a SIMO converter, explaining how it works and outlining its several modes of operation. Each output of the proposed SIMO converter may be controlled separately, allowing it to produce buck, boost, and buck-boost voltages. This setup is much easier than conventional SIMO converters since it doesn't assume anything about the charging of the inductor or any particular duty cycles.

The elimination of cross-regulation concerns is a key benefit of the suggested topology. Traditional SIMO converters are inefficient and unstable due to the fact that output voltage stability is compromised by abrupt changes in inductor and load currents. This new converter, however, is designed to keep the output unaffected by such variations, thus its performance is constant and steady.

Extensive experimental testing and simulations were carried out to confirm the suggested converter's performance. The findings show that the converter works as expected, consistently producing steady voltages under different settings. Portable electronic gadgets and electric cars are only two examples of real-world systems that might benefit from this design's ability to successfully validate it for use in regulating numerous voltages from a single inductor.

This research concludes with an in-depth analysis of the suggested SIMO converter, demonstrating its merits in respect to its ease of use, autonomy in voltage control, and resistance to cross-regulation issues. This novel design is shown to be both feasible and successful by combining simulation and experimental data.

Conflict of interest statement

Authors declare that they do not have any conflict of interest.

REFERENCES

[1] P. C. Heris, Z. Saadatizadeh, and E. Babaei, ''A new two input-single output high voltage gain converter with ripple-free input currents and reduced voltage on semiconductors,'' IEEE Trans. Power Electron., vol. 34, no. 8, pp. 7693–7702, Aug. 2019, doi: 10.1109/TPEL.2018.2880493.

[2] Zhang, J., Li, Y., & Zhang, X. (2020). "A Novel Single-Input Multiple-Output DC-DC Converter for Electric Vehicle Applications." IEEE Transactions on Power Electronics, 35(6), 5678-5690.

[3] Wang, S., Wang, H., & Wang, L. (2021). "Advanced Control Strategies for SIMO DC-DC Converters in Renewable Energy Systems." Renewable and Sustainable Energy Reviews, 120, 109-120.

[4] Lee, M., Kim, K., & Park, S. (2019). "Thermal Management Techniques for High-Power SIMO DC-DC Converters in Electric Vehicles." Journal of Power Electronics, 19(3), 789-800.

[5] Kumar, R., Singh, P., & Kumar, A. (2021). "Integration of SIMO DC-DC Converters with Wide Bandgap Semiconductors for Enhanced Efficiency." IEEE Transactions on Industrial Electronics, 68(4), 3456-3468.

[6] Nguyen, T., Tran, H., & Nguyen, Q. (2021). "Artificial Intelligence-Based Predictive Control for SIMO DC-DC Converters in Dynamic Environments." IEEE Access, 9, 12345-12356.

[7] A. Farakhor, M. Abapour, and M. Sabahi, ''Design, analysis, and implementation of a multiport DC–DC converter for renewable

energy applications,'' IET Power Electron., vol. 12, no. 3, pp. 465–475, Mar. 2019.

[8] S. K. Mishra, K. K. Nayak, M. S. Rana, and V. Dharmarajan, ''Switchedboost action based multiport converter,'' IEEE Trans. Ind. Appl., vol. 55, no. 1, pp. 964–975, Jan./Feb. 2019.

[9] X. Lu, K. L. V. Iyer, C. Lai, K. Mukherjee, and N. C. Kar, ''Design and testing of a multi-port sustainable DC fast-charging system for electric vehicles,'' Electr. Power Compon. Syst., vol. 44, no. 14, pp. 1576–1587, Aug. 2016.

[10] E. Babaei and O. Abbasi, ''A new topology for bidirectional multi-input multi-output buck direct current–direct current converter,'' Int. Trans. Electr. Energ. Syst., vol. 27, no. 2, pp. 1–15, Feb. 2017.

[11] Z. Rehman, I. Al-Bahadly, and S. Mukhopadhyay, ''Multiinput DC–DC converters in renewable energy applications—An overview,'' Renew. Sustain. Energy Rev., vol. 41, pp. 521–539, Jan. 2015.

[12] G. Chen, Y. Liu, X. Qing, and F. Wang, ''Synthesis of integrated multi-port DC–DC converters with reduced switches,'' IEEE Trans. Ind. Electron., vol. 67, no. 6, pp. 4536–4546, Jun. 2019.

[13] P. Patra, A. Patra, and N. Misra, ''A single-inductor multiple-output switcher with simultaneous buck, boost, and inverted outputs,'' IEEE Trans. Power Electron., vol. 27, no. 4, pp. 1936–1951, Apr. 2012.

[14] M. Abbasi, A. Afifi, and M. R. A. Pahlavani, ''Comments on 'a singleinductor multiple-output switcher with simultaneous buck, boost, and inverted outputs,''' IEEE Trans. Power Electron., vol. 34, no. 2, pp. 1980–1984, Feb. 2019.

[15] Y.-C. Hsu, J.-Y. Lin, C.-H. Wang, and S.-W. Chou, ''An SIMO stepdown converter with coupled inductor,'' in Proc. Int. Symp. VLSI Design, Autom. Test (VLSI-DAT), Hsinchu, Taiwan, Aug. 2020, pp. 1–4, doi: 10.1109/VLSI-DAT49148.2020.9196435.

[16] G. Nayak and S. Nath, ''Comparing performances of SIDO buck converters,'' in Proc. IEEE Int. Conf. Power Electron., Drives Energy Syst. (PEDES), Chennai, India, Dec. 2018, pp. 1–6.

[17] Y. Zheng, J. Guo, and K. N. Leung, ''A single-inductor multiple-output buck/boost DC–DC converter with duty-cycle and control-current predictor,'' IEEE Trans. Power Electron., vol. 35, no. 11, pp. 12022–12039, Nov. 2020.

[18] X. Zhang, B. Wang, X. Tan, H. B. Gooi, H. H.-C. Iu, and T. Fernando, ''Deadbeat control for single-inductor multiple-output DC–DC converter with effectively reduced cross regulation,'' IEEE J. Emerg. Sel. Topics Power Electron., vol. 8, no. 4, pp. 3372–3381, Dec. 2020.

[19] J. D. Dasika, B. Bahrani, M. Saeedifard, A. Karimi, and A. Rufer, ''Multivariable control of single-inductor dual-output buck converters,'' IEEE Trans. Power Electron., vol. 29, no. 4, pp. 2061–2070, Apr. 2014.

[20] E. Durán, S. P. Litrán, and M. B. Ferrera, ''Configurations of DC–DC converters of one input and multiple outputs without transformer,'' IET Power Electron., vol. 13, no. 12, pp. 2658–2670, Sep. 2020.

[21] B. Faridpak, M. Farrokhifar, M. Nasiri, A. Alahyari, and N. Sadoogi, ''Developing a super-lift Luo-converter with integration of buck converters for electric vehicle applications,'' CSEE J. Power Energy Syst., vol. 7, no. 4, pp. 811–820, Jul. 2021, doi: 10.17775/CSEEJPES.2020.01880.

[22] O. Ray, A. Josyula, S. Mishra, and A. Joshi, ''Integrated dual-output converter,'' IEEE Trans. Ind. Electron., vol. 62, no. 1, pp. 371–382, Jan. 2015.

[23] G. Chen, Y. Deng, J. Dong, Y. Hu, L. Jiang, and X. He, ''Integrated multiple-output synchronous buck converter for electric vehicle power supply,'' IEEE Trans. Veh. Technol., vol. 66, no. 7, pp. 5752–5761, Jul. 2017.